



HAL
open science

Illusory own body perceptions mapped in the cingulate cortex-An intracranial stimulation study

Irina Popa, Andrei Barborica, Julia Scholly, Cristian Donos, Fabrice Bartolomei, Stanislas Lagarde, Edouard Hirsch, Maria-paola Valenti-hirsch, Mihai Dragos Maliia, Anca Adriana Arbune, et al.

► **To cite this version:**

Irina Popa, Andrei Barborica, Julia Scholly, Cristian Donos, Fabrice Bartolomei, et al.. Illusory own body perceptions mapped in the cingulate cortex-An intracranial stimulation study. *Human Brain Mapping*, 2019, 40 (9), pp.2813-2826. 10.1002/hbm.24563 . hal-02513945

HAL Id: hal-02513945

<https://hal.science/hal-02513945v1>


Submitted on 31 Jan 2025

HAL is a multi-disciplinary open access archive for the deposit and dissemination of scientific research documents, whether they are published or not. The documents may come from teaching and research institutions in France or abroad, or from public or private research centers.

L'archive ouverte pluridisciplinaire **HAL**, est destinée au dépôt et à la diffusion de documents scientifiques de niveau recherche, publiés ou non, émanant des établissements d'enseignement et de recherche français ou étrangers, des laboratoires publics ou privés.

RESEARCH ARTICLE

Illusory own body perceptions mapped in the cingulate cortex—An intracranial stimulation study

Irina Popa^{1,2} | Andrei Barborica^{3,4} | Julia Scholly⁵ | Cristian Donos³ |
 Fabrice Bartolomei⁶ | Stanislas Lagarde⁶ | Edouard Hirsch⁵ | Maria-Paola Valenti-Hirsch⁵ |
 Mihai Dragos Maliia¹ | Anca Adriana Arbune¹ | Andrei Daneasa¹ | Jean Ciurea⁷ |
 Ovidiu-Alexandru Bajenaru^{1,2} | Ioana Mindruta^{1,2} 

¹Neurology Department, University Emergency Hospital Bucharest, Bucharest, Romania

²Neurology Department, University of Medicine and Pharmacy "Carol Davila", Bucharest, Romania

³Physics Department, University of Bucharest, Bucharest, Romania

⁴FHC Inc., Bowdoin, Maine

⁵Neurology Department, Strasbourg University Hospital, Strasbourg, France

⁶Aix Marseille Univ, APHM, INSERM, INS, Inst Neurosci Syst, Timone Hospital, Clinical Neurophysiology, Marseille, France

⁷Neurosurgery Department, Bagdasar-Arseni Hospital, Bucharest, Romania

Correspondence

Ioana Mindruta, MD, PhD, Neurology Department, University Emergency Hospital Bucharest, 169 Splaiul Independenței street, 050098, Bucharest, Romania.
 Email: ioanamindruta@me.com

Funding information

Unitatea Executivă pentru Finanțarea Invatamantului Superior, a Cercetării, Dezvoltării și Inovării, Grant/Award Numbers: COFUND-FLAGERA II-CAUSALTOMICS, COFUND-FLAGERA II-SCALES, PN-III-P1-1.1-TE-2016-0706, PN-III-P4-ID-PCE-2016-0588; European Commission

Abstract

Body awareness is the result of sensory integration in the posterior parietal cortex; however, other brain structures are part of this process. Our goal is to determine how the cingulate cortex is involved in the representation of our body. We retrospectively selected patients with drug-resistant epilepsy, explored by stereo-electroencephalography, that had the cingulate cortex sampled outside the epileptogenic zone. The clinical effects of high-frequency electrical stimulation were reviewed and only those sites that elicited changes related to body perception were included. Connectivity of the cingulate cortex and other cortical structures was assessed using the h^2 coefficient, following a nonlinear regression analysis of the broadband EEG signal. Poststimulation changes in connectivity were compared between two sets of stimulations eliciting or not eliciting symptoms related to body awareness (interest and control groups). We included 17 stimulations from 12 patients that reported different types of body perception changes such as sensation of being pushed toward right/left/up, one limb becoming heavier/lighter, illusory sensation of movement, sensation of pressure, sensation of floating or detachment of one hemi-body. High-frequency stimulation in the cingulate cortex (1 anterior, 15 middle, 1 posterior part) elicits body perception changes, associated with a decreased connectivity of the dominant posterior insula and increased coupling between other structures, located particularly in the nondominant hemisphere.

KEYWORDS

body representation, bodily self-consciousness, intracranial high-frequency stimulation, stereo-electroencephalography, cingulate cortex

1 | INTRODUCTION

The body is an important component of our self and supports our interaction with the environment. Hence, permanent cortical representation of body parts is mandatory at every moment. The way we perceive our body strongly relies on multisensory information, particularly in how this information is integrated into a specific context. Recent reviews have shown the importance of visual, tactile, proprioceptive, auditory or

vestibular input in shaping our body awareness (Azanón et al., 2016) but the underlying functional brain network and the sequence in which the information is processed is still a matter of debate. It is generally agreed (Thurm, Pereira, Fonseca, Cagno, & Gama, 2011; de Vignemont, 2010) that there are different components involved in body representation, mainly the body-schema which is a permanent "unconscious, sensorimotor representation of the body that is invoked in action," that provides information related to location in space, posture and size of body parts and on how these parts form the whole body (Keizer et al., 2013). A second representation of the body is believed to be an occasional

Irina Popa and Andrei Barborica should be considered joint first authors

phenomenon, but conscious one, that includes the conceptual construct of the body based on intellectual understanding and affective, emotional attitude about it which is the body-image (Gallagher, 1986; Keizer et al., 2013). These two processes are in a dynamic relation due to a permanent update by external stimuli. Moreover, there is a growing number of studies trying to understand how the information about our body is integrated into the conscious self and how the body becomes part of our self (Blanke, 2012).

Furthermore, self-related processes, independent on the domain of sensory input (e.g., auditory, visual) activate the medial cortex of the brain, the so called cortical midline structures—CMS (medial orbitofrontal cortex, ventral and dorsal mesial prefrontal cortex, anterior posterior and retrosplenial part of the cingulate cortex and precuneus) across different domains like verbal, spatial, memory and face recognition (Northoff et al., 2006; Northoff & Bermpohl, 2004). Spatial stimuli related to bodily self-processing is further associated to an increased activation of the PCC, medial parietal cortex and subcortical structures. However, changes in the self-identification and first-person perspective induce different activation in most of the CMS including the cingulate cortex as well as in the inferior and middle temporal gyri, right insular cortex and right postcentral gyrus (Murray, Fox, Bzdok, Debban, & Eickhoff, 2014; Northoff et al., 2006; Qin & Northoff, 2011).

On the other hand, much information regarding neural processing of body representation comes from functional imaging studies performed in normal subjects and patients suffering from anorexia nervosa (Bär, de la Cruz, Berger, Schultz, & Wagner, 2015; Gaudio, Wiemerslage, Brooks, & Schiöth, 2016; Hayes et al., 2015; Lee et al., 2014; Mazzoni et al., 2013; Mcfadden, Tregellas, Shott, & Frank, 2014; Mühlau et al., 2007). They have brought into attention the involvement of the cingulate cortex in diseases of body representation like anorexia nervosa.

Consequently, taking into consideration the involvement of the cingulate cortex in processing of self-related stimuli and also in body representation, we hypothesized that the cingulate cortex has a pivotal role in bodily self-consciousness. Therefore, we performed a retrospective study of patients undergoing stereo-electroencephalography (SEEG), investigating changes of body perception induced by high-frequency direct electrical stimulation of the brain at the level of the cingulate cortex. The connectivity of the cingulate cortex associated with the clinical symptoms was evidenced using a correlation method based on calculating the h^2 nonlinear regression coefficient (Wendling, Bartolomei, Bellanger, & Chauvel, 2001) proven to be effective in estimating interdependencies between brain regions (Bartolomei et al., 2017).

2 | METHODS

We have covered large areas of the brain, including some areas that have been showed to be involved in body perception (e.g., temporal, parietal, insular, and peri-sylvian cortex), with intracranial depth electrodes in patients undergoing presurgical evaluation for drug-resistant epilepsy using SEEG (Cardinale et al., 2013; Isnard et al., 2018; Jayakar et al., 2016; Kahane, Minotti, Hoffmann, Lachaux, & Ryvlin, 2003; Munari et al., 1994). Multiple electrodes (9–18) were placed following an individual hypothesis allowing for up to 254 contacts to be recorded in each patient. Electrical stimulation (50 Hz,

5 s) was performed on most of the adjacent contact pairs located on the same implanted electrodes. The current level was gradually increased (up to 3 mA) until a clinical effect was obtained. EEG signals before (10 s) and after (5 s) stimulation were divided into 1-s intervals. Pairwise correlations between all nonstimulated contacts were calculated for EEG signals on each 1-s interval. The magnitude and directionality of the coupling were considered to quantify the functional connectivity between brain areas where multi-contact electrodes are implanted. We have analyzed the changes in the connection's strength and network topology following the application of the electrical stimulation evoking symptoms compared to the baseline.

2.1 | Patients

We selected patients explored by SEEG for phase two invasive presurgical evaluation at the Emergency University Hospital Bucharest and Strasbourg University Hospital between 2000 and 2017. All patients were diagnosed with focal drug-resistant epilepsy and admitted as possible surgical candidates. Therefore, they initially underwent phase one noninvasive presurgical evaluation that included careful patient and family history followed by video-electroencephalography. Consequently, each patient underwent 1.5 or 3 T magnetic resonance imaging (MRI) (isotropic 3D T1, axial and coronal FLAIR and T2, T2* or SWI) and functional imaging (interictal FDG-PET scan). In all patients, invasive exploration using SEEG was considered necessary to delineate the epileptogenic zone (Kahane & Landre, 2008; Munari & Bancaud, 1987) and to map the functional cortex to determine the resection limits.

Structures sampled during SEEG were selected entirely for clinical purpose with no relation to this study or other research intentions. Patients were then selected for this study if they had, at least, one electrode containing contacts outside the epileptogenic zone that sampled any part of the cingulate cortex CC (anterior-ACC, middle-MCC, posterior-PCC). We further excluded patients with cognitive and psychiatric co-morbidities whose condition would interfere with a proper interaction and would therefore question the reliability of the responses.

2.2 | Invasive exploration using SEEG

Each patient underwent SEEG exploration using depth electrodes (Dixi, Besancon, France) having 8 to 18 contacts per electrode, 2 mm contact length, 3.5 mm contact spacing and 0.8 mm diameter. A number between 9 and 18 electrodes were implanted in each patient following an individual hypothesis (Figure 1a,b). The total number of contacts available in each patient was between 112 and 254, of which 64 to 256 (depending on the equipment that has been used over the course of time at the two centers), that were located in the cortical gray matter, were recorded. For Patients 1–7 and 9–10 the electrodes were placed intracranially using the Leksell stereotactic frame (Elekta AB, Stockholm, Sweden). For Patient 8, a microTargeting™ Multi-Oblique Epilepsy STarFix Platform (FHC, Bowdoin, ME; Balanescu et al., 2014; Dewan et al., 2017; Yu, Pistol, Franklin, & Barborica, 2018) was used, while Patients 11–12 were implanted using the ROSA Surgical robot (Medtech, Montpellier, France). To determine

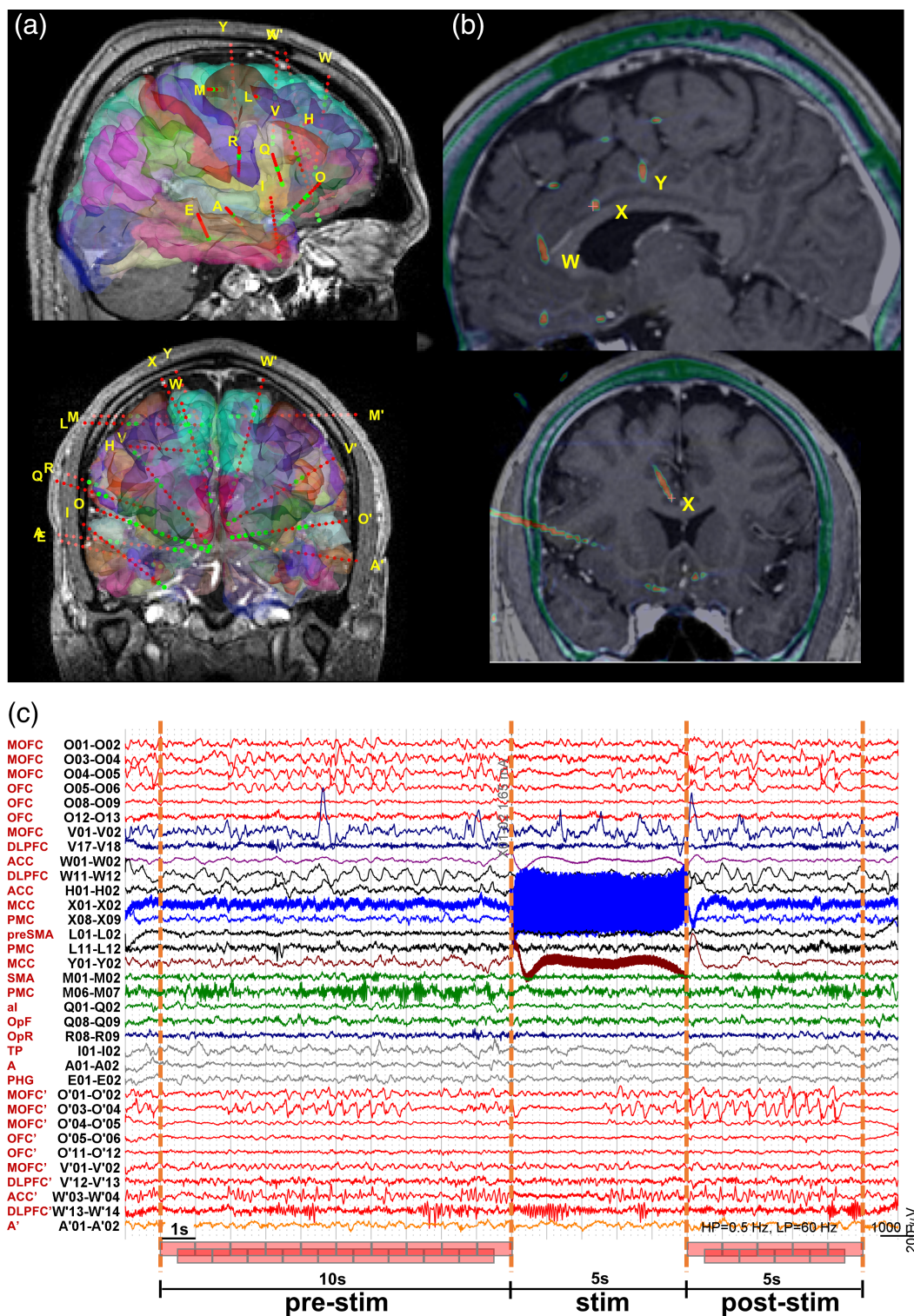


FIGURE 1 (a) Example of an stereo-electroencephalography implantation in Patient 7 using 18 electrodes sampling mainly the right hemisphere (13 electrodes, (A, E, I, O, Q, R, H, V, L, M, X, Y, W), with five electrodes implanted in the left hemisphere (A', O', V', M', W'); 3D maps of implanted contacts, using sagittal and coronal views are shown, superimposed with the FreeSurfer cortical surface reconstruction; the green contacts were included in the recording montage. (b) Sampling of the cingulate cortex in the same Patient 7 using three oblique electrodes (W, X, Y) as visible on the postimplantation CT, blended with T1 MRI (c) high frequency direct brain electrical stimulations performed for 5 s in Patient 7 (S11) on contacts X01-X02 that shows the signal during stimulation, the prestim (10 s) and poststim (5 s) epochs divided into 1-s analysis intervals

the exact location of each electrode and contact, the postimplantation CT scan was co-registered with the preimplantation MRI. Video-SEEG recordings were performed in chronic conditions for 7–14 days at the

University Emergency Hospital Bucharest or the Strasbourg University Hospital using a 64-channel Nicolet Wireless Amplifier or a 256-channel Amplifier (Natus Neuro, Middleton, WI).

All the patients signed a written informed consent in accordance with the Declaration of Helsinki for all the procedures.

2.3 | Direct intracerebral stimulation protocol and data acquisition

Multiple stimulation protocols were carried out routinely as part of the standard presurgical assessment (Trebuchon & Chauvel, 2016) using low frequency 1 Hz (Munari et al., 1993) and single-pulse electrical stimulation (Donos, Mîndruță, Ciurea, Măliia, & Barborica, 2016; Matsumoto, Kunieda, & Nair, 2017), as well as high frequency 50 Hz (HFS; Bernier et al., 1990) direct electrical stimulation; however, only HFS was able to elicit clinical effects of changes in body perception. Therefore, functional mapping of the cortex was systematically reviewed using direct electrical high frequency stimulation of the brain delivered at a rate of 50 Hz (Figure 1c). Bipolar stimulations were performed through pairs of adjacent contacts using a programmable clinical stimulator (Guideline4000LP+, FHC, Bowdoin, ME) in Bucharest and Osirix Cortical Stimulator (Emmendingen, Germany) in Strasbourg with a square, biphasic, 1 ms width pulse for 5 s. In addition, in a subset of patients, resting-state connectivity was calculated based on cortico-cortical evoked potentials elicited by single-pulse electrical stimulation (Supporting Information S1) using the methodology presented in detail in Donos et al. (2016) and Donos, Mîndruță et al. (2016).

Multiple stimulation trials were performed, gradually increasing the current intensity from 0.1 mA to 3 mA, usually in 0.1 or 0.25 mA steps; wider steps of 0.5 or even 1 mA may have been used if repeated anterior stimulations did not elicit any effect. Upper current limit was set by the presence of a clinical or electrical response (after-discharges). Patients were instructed to report any psychological or physical changes they experienced during or after each stimulation. Furthermore, patients were also engaged in different tasks during the stimulation session (e.g., repetitive movements of the limbs to test for motor deficit, reading, counting to test for language or attentional deficits, etc.). Tasks were selected based on the region stimulated. For example, for stimulations included in this study, if the contacts are placed in the proximity of the motor area (primary or secondary), patients were asked to perform a repetitive movement and to count. Tasks have no inter-patient variability. The electrical stimulation was delivered for 1–3 s after the clinical testing started. SEEG signals were recorded at a sampling rate of 4,096 Hz in Bucharest and 1,024 Hz in Strasbourg, and changes in the electrical activity 10 s before and 5 s after the stimulations were analyzed. A new stimulation trial was initiated only after the returning to the baseline pattern of the SEEG trace or after the clinical signs and symptoms had ceased.

For this study, we systematically reviewed all stimulations performed at the level of the cingulate cortex and included in the analysis only sites that elicited changes in body representation. Changes in body representation were defined as any alteration in bodily experience (position, weight, movement) and were categorized as follows: body part transformation, body part displacement, disconnection of one body part from the body (Heydrich, Dieguez, Grunwald, Seeck, & Blanke, 2010). Stimulations at the lowest intensity that evoked a symptom (SYM—target group) were compared with stimulations at typically half the intensity, which did not elicit a symptom

(NS—control group). We excluded all stimulations that triggered after-discharges, auras or seizures.

2.4 | Functional connectivity estimation using nonlinear correlation coefficient h^2

Significant changes in the coupling of SEEG activity in different structures during stimulations that elicited changes in body perception were determined using nonlinear nonparametric regression between pairs of signals characterized by the h^2 correlation coefficient. The h^2 coefficient aims at quantifying the dependency between two neural signals X and Y , independently of the type of relation between them by considering the amplitude of signal Y as a perturbed function of the amplitude of signal X and estimate the variance of this relation (Wendling et al., 2001). The h^2 is bounded between 0 (no correlation) and 1 (maximal correlation) and captures the directionality of the coupling through the asymmetry of the values $h^2_{X \rightarrow Y} \neq h^2_{Y \rightarrow X}$ and the time lag. This computational approach has been shown to be particularly suitable for the analysis of intracranial EEG signals in the context of epilepsy (review in Bartolomei, Lagarde, Wendling, et al. (2017)). In the present study, h^2 values were computed on broadband signals (providing a global estimation of nonlinear interdependencies and used for statistical tests; Bartolomei et al., 2012; Bartolomei, Lagarde, Médina Villalon, McGonigal, & Benar, 2017; Koubeissi, Bartolomei, Beltagy, & Picard, 2014). Since our goal was to determine changes induced by stimulation, we calculated multiple correlation coefficients for each possible combination of nonstimulated pairs of contacts located in the implanted structures for 1-s intervals having a 50% overlap during the following epochs: PRESTIM—10 s before and POSTSTIM—5 s after each stimulation (Figure 1c). HFS trains are applied with at least 40 s pause between them such that the 10 s prestimulation interval was the maximum available during which patients were not engaged in any activity, hence representative for resting state connectivity. A 5 s interval following each stimulation was chosen to be comparable to the prestimulation interval but not too long to diminish the inference of connectivity changes time-locked to the stimulation.

The nonlinear correlation coefficient (h^2) was computed using AnyWave open-source software (Colombet, Woodman, Badier, & Benar, 2015; available at <http://meg.univ-amu.fr/wiki/AnyWave>).

We have selected for analysis contacts located in the gray matter of all structures that were implanted and recorded during video-SEEG. Further analysis of the set of h^2 values, connectivity analysis and graphical representation was performed using Matlab (Natick, MA).

2.5 | Statistical analysis and functional networks characterization

As a measure reflecting the connectivity between pairs of contacts located in the brain structures sampled by the SEEG electrodes, we have calculated the Z -score between the h^2 sets of values, during the PRESTIM and POSTSTIM epochs (Bartolomei et al., 2012; Bartolomei, Lagarde, Médina Villalon, et al., 2017; Koubeissi et al., 2014). The statistical significance of the h^2 differences and associated Z -scores was assessed by performing a Mann–Whitney U -test between sets of responses with a threshold of $p < 0.01$.

The analysis of the h^2 values at the population level was performed using n-way ANOVA with the following 7 factors: (a) patient; (b) structure A and (c) structure B (any of the 51 structures we have labeled); (d) contact X and (e) contact Y (as one structure may be sampled with multiple contacts in the same patient); (f) symptom (to assess if the existence of a clinical effect has any influence) (g) pre/post stimulation (to assess the importance of the stimulation).

By grouping and averaging the h^2 -coefficients at the level of each structure, we were able to calculate the connectivity matrix and plot the connections between structures as circular and 3D graphs.

The subsequent analysis was centered on the differences between two groups: (a) stimulations that exhibited clinical effects related to body perception (target group) and (b) that did not exhibit a clinical effect (control group).

Computational network analysis was performed to determine network measures like the directed h^2 -weighted indegree, outdegree and flow (Rubinov & Sporns, 2010). Indegree has been calculated as the number of incoming connections to a node weighted by the h^2 values (also referred to as instrength), thresholded using the third quartile of the h^2 -coefficient values during the POSTSTIM epoch, outdegree as the number of weighted outgoing connections from a node (also referred as outstrength), while the flow represents the difference between the indegree and outdegree. Analysis was performed separately for each structure, in the PRESTIM and POSTIM epochs, for the SYM and NS trials.

2.6 | Data representation

Cortical surface reconstructions were performed using FreeSurfer software package (Fischl, 2012; available at <http://surfer.nmr.mgh.harvard.edu>) for the eight patients investigated in the Bucharest center. Using the method of Dale, Fischl, and Sereno (1999) and Fischl, Sereno, and Dale (1999), reviewed in Winkler et al. (2012), population-level analysis of the contacts' topography was performed by mapping the individual contacts to the cortical surface reconstruction of each patient, then projecting them on a spherical surface model, followed by pooling across patients and projection back to the FreeSurfer *fsaverage* template. For the four patients investigated in the Strasbourg center we used the anatomical contact coordinates inferred from patient's MRI and projected them on the Free Surfer's *fsaverage* template. We defined as the cingulate cortex, the following anatomical regions: the cingulate gyrus, the cingulate sulcus including the marginal branch, isthmus of the cingulate gyrus. We further divided it in three parts: anterior cingulate cortex (ACC) that includes the subcallosal and pregenual part with the posterior border the vertical line drawn through the anterior commissure. Middle cingulate cortex (MCC) is delimited by the two vertical lines that pass the anterior and the posterior commissure and the posterior cingulate cortex (PCC) that lies posterior to the vertical line passed through the posterior commissure. In particular, labeling of the individual stimulation locations was performed based on the automatic parcellation of the cortex performed by the FreeSurfer package, using the Destrieux, Fischl, Dale, and Halgren (2010) anatomical nomenclature: area 6 was considered as ACC, areas 7, 8, and 46 as MCC, while 9 and 10 as PCC.

3 | RESULTS

We reviewed stimulations from 110 patients in which the cingulate cortex was sampled and functionally mapped and included 12 right-handed patients where changes of body perceptions were obtained: 8 patients were explored in the Bucharest center and 4 in Strasbourg. Nine (75%) patients had an epileptogenic zone located in the frontal lobe, one in the temporo-basal region, one insular-opercular and one insular. Usual seizure semiology did not include any symptoms or signs similar to those elicited by stimulations included in this study. 83.3% of the patients underwent resective surgery and 50% are seizure-free (Engel I mean follow-up 35 months). Two patients (Patients 4 and 11) refused open brain surgery after invasive exploration (Table 1). In these patients the epileptogenic zone was delineated based on the electroclinical correlations and did not overlap with the stimulated locations.

3.1 | Clinical effects

From a total of 412 stimulated cingulate cortex sites, 17 elicited clinical effects consistent with illusions of body perception (Table 2). These clinical effects involved a limb, the head, a hemi-body (right or left, upper or lower part) or the entire body. In five stimulations (S5, S7, S13, S15, and S16) patients reported the feeling that part of the body becomes *heavier/lighter* with no motor deficit associated. These sensations involved the right or the left upper limb, contralateral to the side of the MCC stimulated. Additionally, Patient 13 explained that, associated to this feeling, he also experienced pain located at the level of the right upper limb. A second clinical effect consisted in the *sensation of being pushed/pulled upwards/backward*; these sensations were reported in four stimulations (S3, S8, S9, S10) performed at the level of the MCC and were noted to affect the ipsilateral limb or the entire body. The direction of the shift was contralateral to the side of stimulation when the entire body was affected and was to the back when only a limb was involved. Two patients reported *illusory sensation of movement*: Patient 11 told that he felt like the upper part of the body entirely moved to the ceiling while the right MCC was stimulated and Patient 14 reported that "he feels like the right upper limb moves to the left" while the right PCC (contralateral to the limb involved) was stimulated. There were two patients that reported a *sensation of pressure* located at the upper extremity in Patient 4 and the entire body in a descending manner in Patient 7, S11. During this stimulation, performed in the ACC, fear was associated to the feeling of pressure when it involved the chest region, near the heart. We therefore believe that the fear is a symptom triggered by the fact that the strange sensation of pressure involves the anterior chest region and is not generated by stimulation per se. There were 4 patients that described unique sensations during HFS of the MCC. Patient 1 reported that "it seems like the left part of the body floats," sensation that affected the hemi-body contralateral to the stimulation side, Patient 2 noted a sensation of decomposition with the feeling that "the left lower limb detaches from the body and loses it" and Patient 3 said that he feels like distal hand muscles belonging to the thenar eminence contract but no movement of the hand or of the fingers was noted. Lastly, Patient 7 (stimulation 12) reports the feeling that

TABLE 1 Demographic data of the patients included in the analysis, location of the epileptogenic zone, surgical outcome and pathology

Patient	Sex	Age	Epileptogenic zone	Lateralization	Pathology	Number of electrodes	Number of contacts	Implantation side	Surgical outcome
1	F	11	Frontal	R	FCD IIA	16	205	Right	Engel IA
2	F	36	Insular-opercular	R	FCD IIB	15	205	Right	Engel IA
3	M	29	Frontal	R	FCD IIB	9	112	Right	Engel IID
4	M	28	Frontal	L	Not operated	15	188	Bilateral	
5	M	42	Frontal	L	FCD IIA	13	155	Bilateral	Engel IA
6	M	28	Frontal	R	FCD IIA	13	173	Bilateral	Engel IVB
7	M	38	Frontal	L	FCD IIA	18	254	Bilateral	Engel IA
8	M	20	Frontal	R	FCD IIA	16	208	Bilateral	Engel IA
9	M	23	Frontal	R	Normal	16	192	Bilateral	Engel IVA
10	F	24	Insular	L	FCD IIA	14	197	Left	Engel IVA
11	M	11	Frontal	L	Not operated	13	160	Left	
12	F	31	Temporo-basal	R	Normal	11	135	Right	Engel IC

his head is turning to the right (ipsilateral to the side of stimulation) and that it will detach from the neck followed by a visual hallucination that he can see himself from outside, from all angles without the existence of a secondary body.

There were multiple stimulation trials (typically 2–3) in each patient to assess the reproducibility of the symptoms as well as sham stimulation trials (0 mA) to rule out psychogenic events. Description of body perception changes were consistent across stimulation trials within subject and also between subjects that reported the same kind of illusions (changes in weight, sensation of being pushed, illusion of movement, or sensation of pressure). In addition, patients were asked to subjectively compare the intensity of the sensation (stronger or lighter) as a function of the intensity of the applied current. However, SEEG data was only analyzed from trials that elicited changes of body perception at the lowest intensity.

In nine stimulations, the clinical effect was contralateral to the side of stimulation, in four the sensation was ipsilateral and during four stimulations the sensation was bilateral or involved the axial part of the body (head or trunk).

In these patients in which stimulation of the cingulate cortex elicited changes in body perception we have reviewed all stimulations that were performed at the level of all structures implanted. We have found several effects that might be related to illusory body perception: sensation of pressure/constriction/being pushed (P1–S and OpP, P2–DLPFC, P7–al), sensation like something covers the left hemibody (P3–OpP), like “touching a flower” (P4–al) or sensation that the left leg falls (P7–SMA). In Patients 5, 6, 8, 9, 10, 11, and 12, no other regions elicited symptoms of body-perception while being stimulated.

3.2 | Brain regions analyzed

All patients included in the analysis were MRI negative, there was no lesion visible on their MRI. There were 51 structures sampled by SEEG electrodes and the following were included in the analysis (Figure 2c,d). ACC (anterior cingulate cortex), MCC (middle cingulate cortex), DLPFC (dorsolateral prefrontal cortex), DMPFC (dorsomesial prefrontal cortex), MOFC (mesial orbitofrontal cortex), OFC

(orbitofrontal cortex), STG (superior temporal gyrus), MTG (middle temporal gyrus), A (Amygdala), Hc (Hippocampus), preSMA (presupplementary motor area), SMA (supplementary motor area), PMC (premotor cortex cortex), R (primary motor area), S (primary somatosensitive area), OpF (frontal operculum), OpR (rolandic operculum), OpP (parietal operculum), al (anterior insula), and pl (posterior insula) were sampled bilaterally. On the right side we included additional structures: AG (angular gyrus), F (fusiform gyrus), SMG (supramarginal gyrus), O (lateral occipital cortex), OpT (temporal operculum), PCC (posterior cingulate cortex), PHG (parahippocampal gyrus), ITG (inferior temporal gyrus), SPL (superior parietal lobule) and TP (temporal pole). The VMPFC (ventromesial prefrontal cortex) was sampled only on the left side. At individual level, six patients were explored using bilateral hypothesis, in four patients we sampled only the right hemisphere and in two patients only the left one. The structures in the left hemisphere are marked with an apostrophe. Of the 2,601 possible connections between these structures, 710 (27.3%) structure pairs were explored in at least one patient. There were 522 intrahemispheric pairs of structures analyzed (190 in the left hemisphere and 332 in the right hemisphere) and 188 pairs of structures that assessed interhemispheric connections.

There were 15 stimulations performed at the level of MCC, one at the level of PCC and one at the level of ACC (see Table 2 and Figure 2).

3.3 | Functional connectivity

We performed connectivity analysis using nonlinear regression (h^2) on SEEG data from all 12 patients; h^2 values were calculated for 31 stimulations: 17 stimulations that elicited a clinical effect (interest group) and 14 stimulations with no clinical effect elicited (control group). Patients P1, P7, and P12 had no control stimulations available. The mean current intensity during stimulations in the interest group was 1.121 mA and 0.607 mA in the control group.

A total number of 1,110,720 h^2 values (median value of 0.22, Figure 3) were included in the statistical analysis: 607740 symptom, 502,980 no-symptom, 779,472 prestim, 331,248 poststim, in 12,272

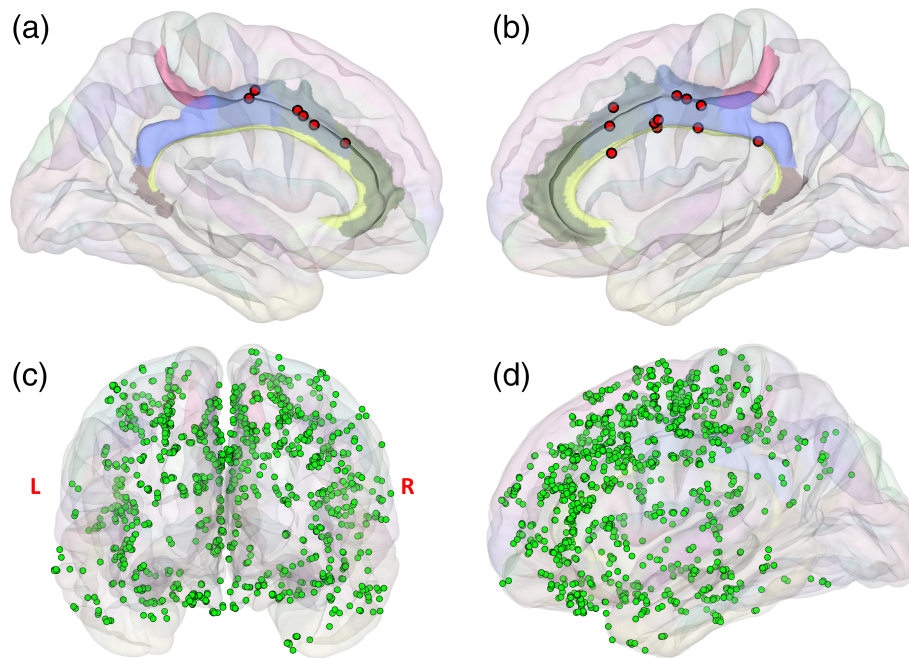


FIGURE 2 (a,b) Location of the stimulation sites that elicited clinical responses related to body perception co-registered across patients and represented on the FreeSurfer *fsaverage* template. The cingulate areas 6,7,8,9,10, and 46 from the Destrieux atlas (Destrieux et al., 2010) have been highlighted; (c,d) location of the recording sites, shown on the *fsaverage* glass brain

contact pairs of 162 electrodes, 25 intervals per contact pair ($X - Y$), 2 groups (SYM/NS) and two values h_{XY}^2, h_{YX}^2 corresponding to the correlation $X \rightarrow Y$ and $Y \rightarrow X$. Multifactorial n-way ANOVA evidenced the fact that all factors significantly modulated the h^2 -coefficient values.

The analysis at the structure level shows 218 (8.7%) pairwise correlations significantly enhanced in SYM versus NS conditions

($p < 0.01$), and 142 (5.7%) pairwise correlations were significantly weaker in SYM versus NS ($p < 0.01$).

3.4 | Network characterization

We have characterized the changes in broadband connectivity at the level of the entire patient population by analyzing a set of 44,678 Z-scores for

TABLE 2 Location of contacts stimulated in each patient, current intensity and details regarding clinical symptoms

Patient	Stimulation	Location	Intensity (mA)	Distribution	Lateralization	Notes
1	S1	MCC	1	Hemibody	Contralateral	Sensation of floating of the left hemibody
2	S2	MCC	0.75	Lower limb	Contralateral	Sensation that the lower limb detaches from the body, loses it
3	S3	MCC	1	Hemibody	Contralateral	Sensation that the body is being pushed to the left
4	S4	MCC	1.25	Head	Bilateral	Sensation of pressure in the top of the head
5	S5	MCC	0.66	Upper limb	Contralateral	Sensation that the upper right limb is heavier
5	S6	MCC	0.75	Upper limb	Contralateral	Sensation that distal hand muscles contract
5	S7	MCC	0.25	Upper limb	Contralateral	Right upper limb feels lighter
6	S8	MCC	0.75	Upper limb	Ipsilateral	Feels that the right hand is pulled from behind
6	S9	MCC	0.75	Upper limb	Ipsilateral	Feels that the right hand is pulled from behind
6	S10	MCC	1.25	Upper limb	Ipsilateral	Feels that he is pushed backwards
7	S11	ACC	1.65	Face+trunk	Bilateral	Sensation of pressure that starts at the face and descend in the entire body and fear when it arrives at the heart level
7	S12	MCC	2	Head	Bilateral	Sensation that the head turns to the right side, that the head will explode, will detach from the neck, sees himself from outside
8	S13	MCC	1	Upper limb	Contralateral	Sensation that the left upper limb becomes heavier
9	S14	MCC	2	Trunk	Bilateral	Sensation that the upper part of the body moves upwards
10	S15	MCC	1	Upper limb	Contralateral	Sensation that the right hemibody and all the head become heavier
11	S16	MCC	2	Upper limbs	Contralateral	Sensation that the upper right limb becomes heavier associated to pain
12	S17	PCC	1	Upper limb	Ipsilateral	Sensation that upper right limb moves to the left side

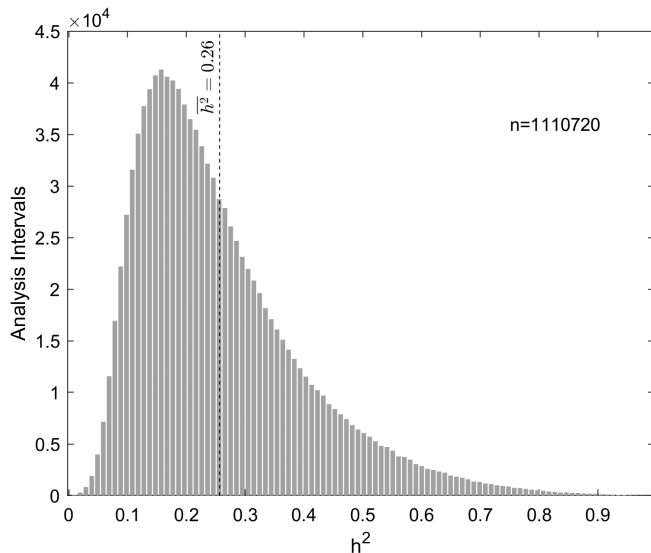


FIGURE 3 Distribution of the $n = 1,110,720$ values of the h^2 coefficients for each analysis interval included in the analysis, 607,740 symptom, 502,980 no-symptom, 779,472 prestim, 331,248 poststim, in 12,272 contact pairs of 169 electrodes, 25 intervals per contact pair, two groups (SYM/NS) and two values (h_{XY}^2, h_{YX}^2)

the h^2 values in the POSTSTIM interval vs PRESTIM interval. There were 1,361 out of 20,134 significant ($p < 0.01$) Z-scores for stimulations not evoking clinical symptoms (mean Z: 2.29 ± 2.27) and 1,300 out of 24,544 significant ($p < 0.01$) Z-scores for stimulations evoking clinical symptoms (mean Z: 0.89 ± 1.87). The Z-scores related to the comparison of pre- and poststimulation h^2 values in each group (control and interest) among all patients are shown in Figure 4.

Further analysis of SEEG trace implied a comparison of previous (pre- and poststimulation) results from control and interest groups to determine significant changes in the coupling of structures when the clinical effect was elicited. An example of changes in connectivity induced by HFS for patient P3 is shown in Figure 5. It may be observed that HFS of the MCC results in a decoupling between the pl and DLPFC, SPL and MCC as well as ACC and DLPFC.

Changes of connections between the two conditions (SYM/NS) at a structure level have been calculated. The adjacency matrix in Figure 6 that contains all 51 brain structures analyzed, displays significant changes marked with “*.” There is a clear disconnection of the pl’ and to a lesser extent of the al’ mainly from the ACC’, MCC’ but also from DMPFC’, DLPFC’, SMA’, PMC’, R’, S’, OpF’, OpP’ and between the two insular subdivisions (al’ and pl’) with a maximum h^2 value of 0.5. On the other hand, in the nondominant hemisphere, there is an increase in connectivity between the preSMA and MOFC, DMPFC, DLPFC, ACC, SMA, S, TP, the OpF and R; al and SMA; pl and ACC, PCC; DLPFC and ACC. One can note an interhemispheric reorganization of connections with a clear increase in h^2 values between F and Hc’ but also between F and ITG and the MOFC’, DLPFC’, preSMA’, SMA’, PMC’, A’, Hc’, MTG’, STG’, OpP’, OpR.’ There is also an increased connection of the ACC, MCC, preSMA, R, and ACC’, preSMA’, SMA’, PMC, R’ with maximum h^2 values between 0.3 and 0.4.

We performed a group-level analysis focused on determining network reorganization between the SYM and NS conditions. Figure 7 displays the comparison between control and interest group where

we can see that a SYM condition is generally associated with a decrease in the number of connections in the left hemisphere, excepting VMPFC’, MOFC’, and OpF’ that exhibited an increase in connectivity. By contrast, the right hemisphere shows several hubs of increased connectivity ACC, MCC, SMA, R, S, F, MTG, ITG, al, pl, O, while a decrease of connectivity can be observed in the MOFC, A, Hc, OpF, and PCC.

4 | DISCUSSION

Our study attempts to highlight the reorganization of the brain networks underlying the illusory body perceptions elicited by direct electrical stimulation of the cingulate cortex (Figure 2). Previous studies described similar complex illusory body perceptions in the form of bilateral sensations of levitation while stimulating the medial parietal cortex around the subparietal sulcus (Richer, Martinez, Robert, Bouvier, & Saint-Hilaire, 1993) but no reference was made to the corresponding network. In addition, disorders of body representation have been studied in patients with epilepsy that present alteration of body perception (sensation of being shifted backward, sensation of the body being invaded by a stranger, diminished awareness of body signals from the trunk or limbs) that were matched with lesions in different brain areas like right intraparietal sulcus, right SMA and superior frontal gyrus (Heydrich et al., 2010), right posterior parietal cortex (Nightingale, 1982) or right posterior occipito-parietal cortex (Gloning, Gloning, Jellinger, & Tschabitscher, 1963). We consider as strengths of our study the fact that (a) we found 17 instances of rare illusions of body perception that could relate to bodily self-consciousness by affecting self-identification (Blanke, 2012), (2) highlights, for the first

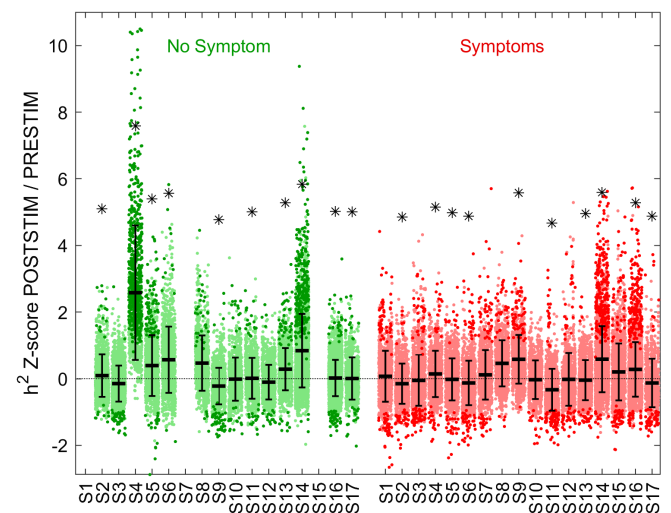


FIGURE 4 Z-score of the h^2 values in the POSTSTIM epoch, compared to the PRESTIM epoch for each stimulation, for the control (NS) and interest (SYM) groups; the Z-scores for individual pairs of signals that had a p -value less than 0.01 (Mann–Whitney U -test) are represented using dark colors, while the nonsignificant ones are represented using light colors; means and SDs of the Z-scores for each stimulation are shown in black and significant differences between the mean scores in SYM and NS conditions are marked with a *sign (Mann–Whitney U -test $p < 0.01$)

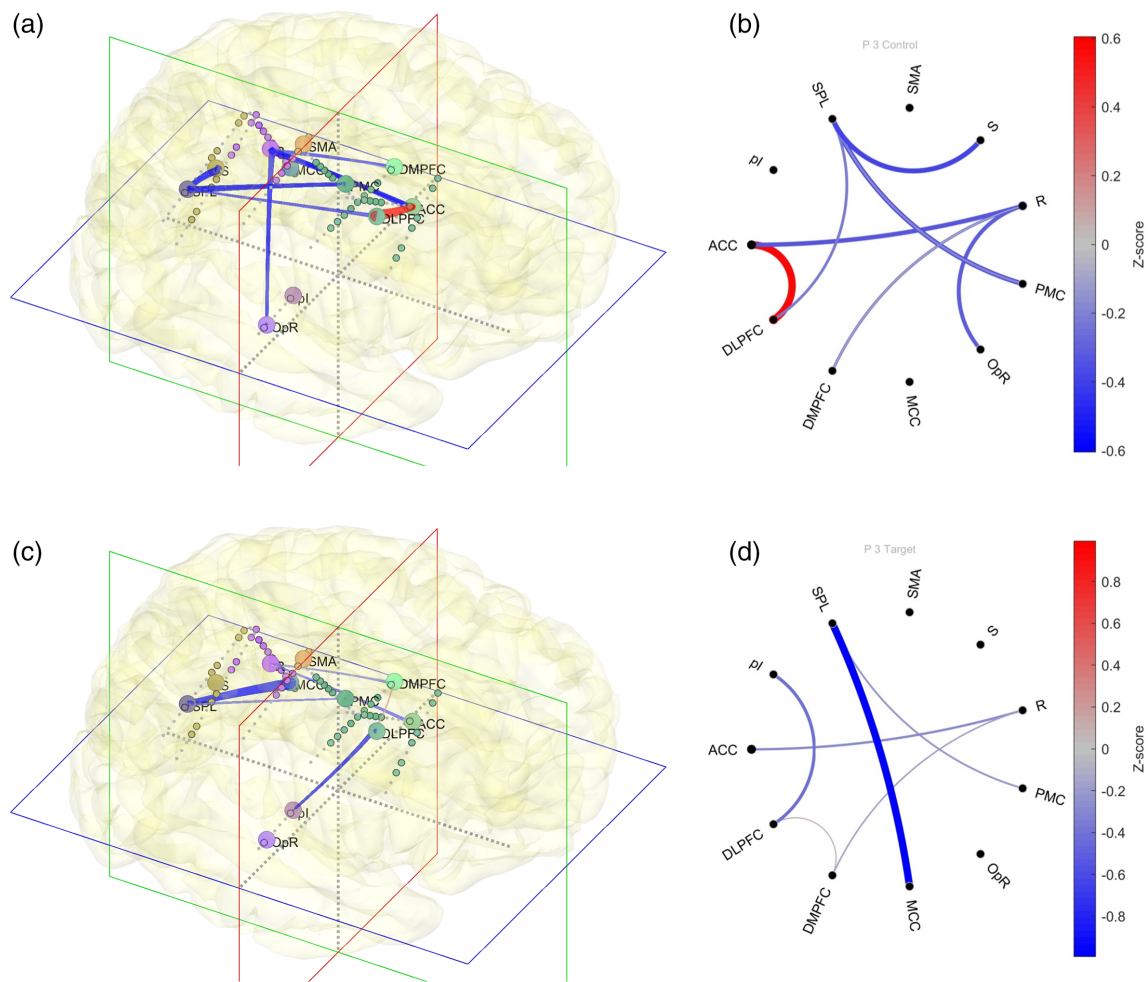


FIGURE 5 Changes in connectivity between brain structures as a result of electrical stimulation in Patient 3. Z-scores of the h^2 changes in the POSTSTIM vs PRESTIM epochs for the control (a,b) and interest (c,d) trials, represented in 3D (a,c) and as circular graphs (b,d); increased connectivity is represented using red colors, while decreased connectivity is shown in blue; the thickness of the lines is proportional to the magnitude of the variation in connection strength; a weaker coupling can be observed between the posterior insula and dorsolateral prefrontal cortex (DLPFC) and between superior parietal lobule, middle cingulate cortex, anterior cingulate cortex, and DLPFC

time, the involvement of the cingulate cortex in body representation, (3) characterizes the functional networks underlying this process.

From a clinical point of view, we elicited changes in perceptions of weight, position, motion or muscle contraction in different parts of the body (Table 2), which could be due to changes of proprioception. Proprioception is a complex somatosensory modality that enables humans to know where parts of their body are located and to be aware of their movement at any moment (Sherrington, 1911). The fact that these clinical effects are the result of a failed integration of proprioceptive information could be supported by electrical data that reveal a decrease in both instrength and outstrength of the posterior dominant insula (Figure 7). Stimulation 3 (patient reports that the contralateral upper limb becomes heavier) is an example of how the pl' decouples from the DLPFC' (Figure 5c,d). Since it has been previously proven that the cingulate and insular cortex are connected (Donos, Mäläia, et al., 2016), we could hypothesize that HFS of the CC induced a functional disconnection of the dominant pl (Figure 6) which is a hub for the integration of multisensory modalities (Rodgers, Benison, Klein, & Barth, 2008; Zu Eulenburg et al., 2013). In addition, posterior dominant insula has been shown to be part of the network involved in

bodily self-consciousness illusions, namely heautoscopy, an unstable representation of self-identification, self-location and the first-person perspective (Heydrich & Blanke, 2013). In addition, Blanke et al. reports out of body experience and autoscopic hallucination accompanied by vestibular sensation (floating, elevation, vertigo, falling, sinking, lightness, or heaviness) related to epileptic seizure semiology or elicited during direct brain stimulation of the temporo-parietal junction--TPJ (Blanke, Landis, Spinelli, & Seeck, 2004). In five out of the six patients, the visual and nonvisual phenomenology of illusions of body perception were part of the habitual seizure semiology generated by the activation of the epileptogenic network so probably more than only the TPJ was involved. However, in one patient (Blanke, Landis, Seeck, & Roger, 2002), OBE were elicited during HFS of the TPJ but using a different invasive approach by subdural electrodes which permits stimulation of a more extensive cortical area than the SEEG electrodes. Also, OBE phenomena were elicited during a stimulation above the threshold intensity of the same area that initially elicited vestibular sensations of falling or sinking. This could mean that the TPJ is a hub in the network involved in processing body related information and that this network could be activated by high

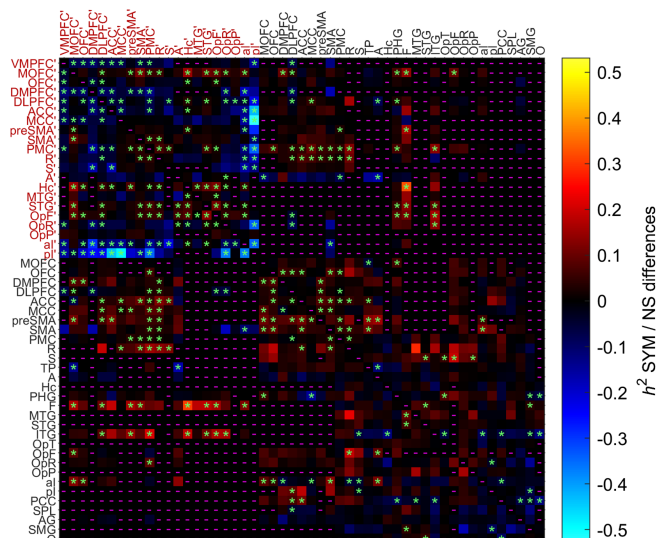


FIGURE 6 Poststimulation h^2 comparison between control (NS) and interest (SYM) stimulation trials, represented as a connectivity matrix in which the differences between the means of the directed h^2 values in the SYM/NS conditions are represented for each structure pair. In this analysis, contacts have been grouped according to their parcellation labels. Elements marked with a green * have n -way ANOVA p -value associated with the symptom factor, for the subset of h^2 values corresponding to each pair of structures, less than 0.01. Pairwise connections marked with a magenta dash have not been sampled with electrodes

stimulation levels applied to other hubs. Moreover, our network analysis reveals changes in connectivity associated to clinical effects which involved the dominant insula and temporo-basal nondominant regions (Figure 7). A general overview of the network highlighted by HFS and h^2 analysis is presented in Figures 6 and 7. We observe a decoupling of left-side structures (mainly the pl' as already mentioned) and increased coupling between right-side brain structures' networks, namely frontoparietal and inferior temporal. This has been previously reported in fMRI studies by Amemiya and Naito (2016); they found that the right inferior frontoparietal regions (frontal operculum, anterior insula, middle frontal gyrus, orbitofrontal cortex, inferior parietal cortices) play a dominant role in corporeal awareness. The connectivity analysis reveals an increase in the number of degrees/strength in OFC, OpF, al, and OpP (Figure 7), in agreement with previous studies (Amemiya & Naito, 2016), as well as an increase in the connectivity of the right fusiform gyrus and ITG, which are part of the ventral occipitotemporal pathway. Studies have shown the existence of a selective fusiform body area (FBA; Schwarzlose, 2005) besides the classical extrastriate body area (EBA), with right side dominance that responds selectively to body-related stimuli. Individual structure analysis shows that connection changes in this hub are mainly due to its increased coupling with the MOFC,' DLPFC,' MCC,' preSMA,' SMA,' Hc,' OpF,' and STG' (Figure 6), most of them involved in the ventral visual pathway framework of object quality (Kravitz, Saleem, Baker, Ungerleider, & Mishkin, 2013). Could this increased flow of visual information be an over-response to unclear proprioceptive information induced by stimulation?

Furthermore, functional brain imaging (positron-emission tomography—PET) studies concerning changes in body-schema using rubber hand

illusion (Tsakiris, Hesse, Boy, Haggard, & Fink, 2007) were able to determine an increased PET signal in the right posterior insula similar to our results (Figure 7). We were additionally able to determine that, at the group-level, nondominant pl is a projector and further delivers the information to the DLPFC (Figure 6). The DLPFC is, in turn, a stable hub that does not show any change in connectivity (Figure 7). This could be a pathway through which body-related information become consciousness. There is further evidence of this point that comes from patients with somatoparaphrenia with lesions in the right pl (Blanke, 2012).

Several patients in our group described illusory motion sensation (e.g., stimulation 17 “I feel that my upper right limb moves to the left side”) that could be classified as sense of agency, a cognitive process that accepts the ownership of the movements (Murata, Wen, & Asama, 2016). A match between the map of the planned movement and the feedback from somatosensory information determines whether the action is accepted as own (Blakemore, Frith, & Wolpert, 1999). There are various animal studies supporting that this feedback loop is processed at the level of the anterior intraparietal (Ishida, Nakajima, Inase, & Murata, 2010) or inferior parietal cortex (Chambon, Wenke, Fleming, Prinz, & Haggard, 2013; Farrer et al., 2008) reviewed in Murata et al. (2016). Hence, the fact that we found a significant change in connections at the level of the S and PMC, bilaterally, (Figure 7) could be due to continuous involvement of this network in processing the sensations induced by stimulation as related to the own body. The PMC has also been largely involved in body representation because of its bimodal neurons that integrate visual and proprioceptive information. These neurons could also be found in the intraparietal sulcus (Graziano & Botvinick, 2002). One peculiar difference that we found is that even though we analyzed the SPL, AG, and SMA, we did not find any significant changes in connections at a group-level analysis (Figure 7). However, patient-level analysis highlights a decrease of coupling between the SPL and MCC (Figure 5). One explanation could come from the statistical threshold as the SPL was sampled only in two patients. In Supporting Information S1 we present resting-state connectivity of the MCC in Patients 2 and 3 using another modality, based on cortico-cortical evoked potentials, highlighting connections between the MCC and several parietal regions (SPL, temporo-parieto-occipital junction—TPO and precuneus—PrC). It seems that resting state connectivity pattern between the MCC and parietal cortex is altered when illusory body perceptions are elicited though a decrease in coupling between the two regions.

To our knowledge, there are no other neurophysiological studies to introduce the involvement of all parts of the cingulate cortex in body awareness. However, indirect evidence comes from imaging studies performed in anorexia nervosa, which is believed to be determined by a distorted cortical representation of the body (Keizer et al., 2013). Structural (Mühlau et al., 2007) and functional (Bär et al., 2015) MRI studies reveal changes in the cingulate cortex in this pathology indicating a possible role that the cingulate cortex might play in body representation. In relation to this, here we report stimulations in the cingulate cortex (Figure 2) that induce significant changes in connections in the ACC, MCC, and PCC that subsequently elicit body displacement perceptions. Furthermore, our study demonstrates that complex body illusions can be evoked by direct electrical stimulation of this region. A recently published study (Caruana et al., 2018)

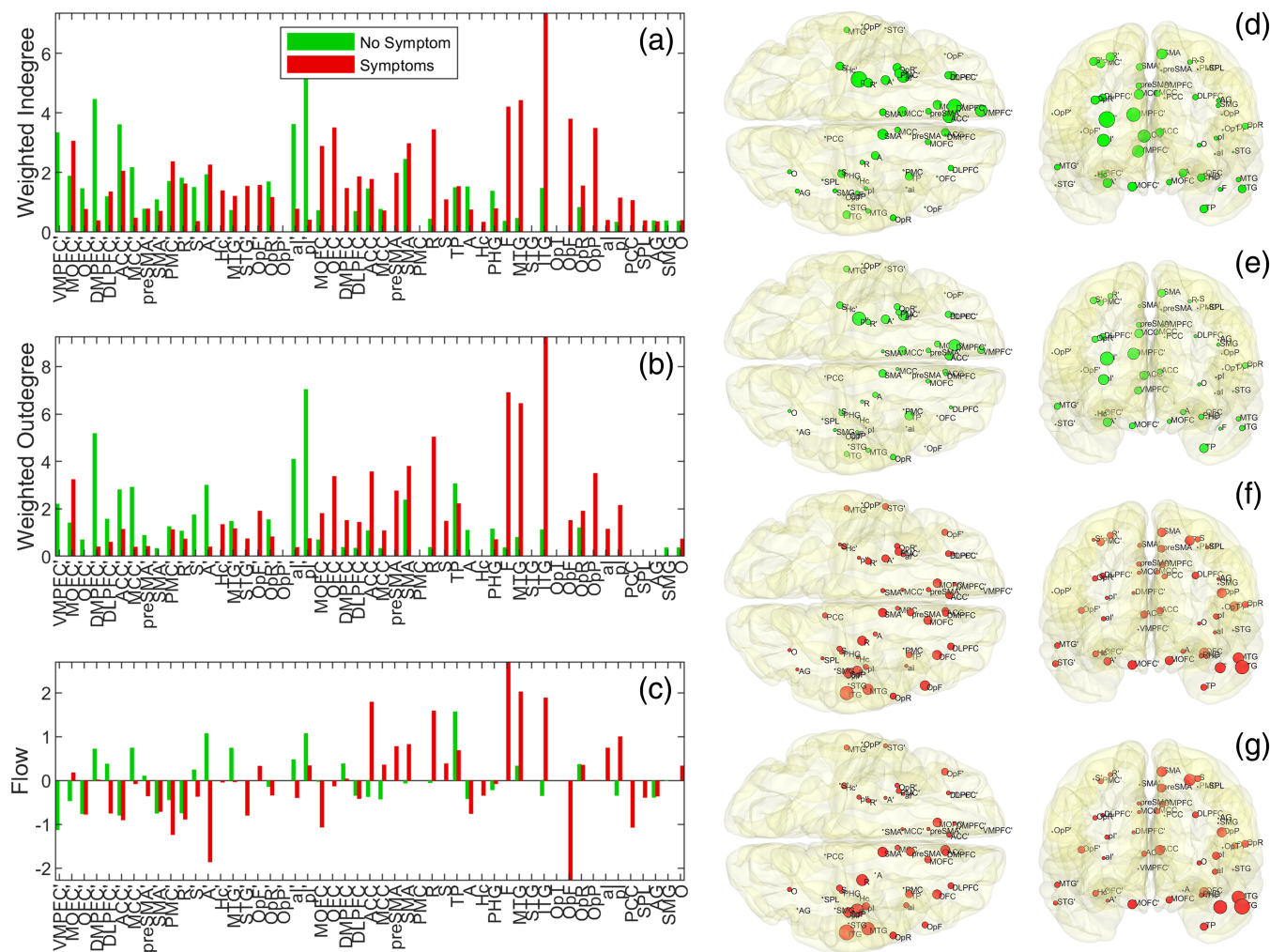


FIGURE 7 Network measures for the set of 51 structures in 12 patients. Only h^2 values within the third quartile of the poststimulation set were included in this analysis; (a) weighted indegree (instrength); (b) weighted outdegree (outstrength); (c) flow; right panels (d–g) show node degrees as spheres having a radius proportional to the network measure, represented at the structures' 3D location on the *fsaverage* glass brain, in axial and coronal views; (d,e) indegree, (f,g) outdegree, (d,f) no-symptom; (e,g) symptoms; the structures in panels (a–c) are grouped by hemisphere and follow an anterior–posterior ordering

thoroughly mapped the cingulate responses to electrical stimulation in 329 patients, but none of the symptoms we did find were reported and no per-patient functional connectivity analysis was performed. However, Caruana et al. report in their paper vestibular responses as “sensation of falling” and several miscellaneous responses that could include clinical effects similar to illusory body perceptions without being individually reported. Being such rare symptoms, it may be possible that they were not assigned a separate category. Cingulate cortex thus appears to be a critical hub in the body perception network connecting the posterior insular cortex with the spatial exploration network. This might have implications both on a physiological and at a clinical level. Although further investigations are needed, our study could point to an early semiology indicating cingulate epilepsy, along with emotions, laughter and hypermotor behavior. This was suggested in the case series reported by Alkawadri et al. (Alkawadri, So, Van Ness, & Alexopoulos, 2013).

There are several limitations of our study that come from the general method used (space-resolution limitation due to limited cortical coverage and no clear control over the subjective clinical effects).

Limited assessment of this kind of complex clinical responses related to body-awareness which were not specifically quantified (e.g., visual-analog scales) is another limitation. High-frequency intracranial stimulation evokes tens or hundreds of different clinical responses, ranging from very predictable and reproducible to very rare and sometimes unexpected symptoms. Therefore, it is almost impossible to predefine a test, that would have required a significant set of reproducible prior observations, for the less frequent responses. Nevertheless, there are considerable reports of uncommon clinical effects elicited by intracerebral stimulation on small sample size (Blanke et al., 2002; Parvizi, Rangarajan, Shirer, Desai, & Michael, 2014; Picard, Scavarda, & Bartolomei, 2013; Quraishi, Benjamin, Spencer, Blumenfeld, & Alkawadri, 2017; Yu et al., 2018). The variable spatial sampling across patients and structures directly affect the number of probed connections, and particularly the connectivity graphs presented in Figure 7. We have analyzed electrical signal 5 s after each stimulation (see also (Bartolomei et al., 2012; Bartolomei, Lagarde, Médina Villalon, et al., 2017) and not during the HFS. This would have been impossible due to the stimulation artifact. The temporal resolution of the 5-s epoch is

not able to capture the time course of the complex physiological processes; however, it is comparable to fMRI's temporal resolution and might still be one of the best available tools for probing causal processes in the brain (Rizzolatti, Fabbri-Destro, Caruana, & Avanzini, 2018).

5 | CONCLUSIONS

HFS at the level of the cingulate cortex reconfigures brain networks related to changes in body perception. Cingulate cortex integrates multisensory interoceptive and exteroceptive information regarding body parts location, shape, weight and self-identification. Our network analysis has shown that stimulation induces a disconnection of the left posterior insular cortex and activates the connections of the right hemisphere, particularly of the ventral visual stream and frontoparietal inferior cortex.

ACKNOWLEDGMENTS

The authors would like to thank Alin Rasina MD, who was part of the functional neurosurgery team, for his help with intracranial electrodes placement. This work was supported by Romanian UEFISCDI research grants PN-III-P4-ID-PCE-2016-0588, PN-III-P1-1.1-TE-2016-0706 and European Union COFUND-FLAGERA II-SCALES and COFUND-FLAGERA II-CAUSALATOMICS.

CONFLICT OF INTERESTS

Dr Andrei Barborica is a Vice-President and Chief Technological Officer of FHC Inc, the manufacturer of the electrical stimulator and stereotactic fixture used at the Bucharest center. The other authors have nothing to disclose in relation to this work.

ORCID

Ioana Mindruta  <https://orcid.org/0000-0001-9329-5132>

REFERENCES

- Alkawadri, R., So, N. K., Van Ness, P. C., & Alexopoulos, A. V. (2013). Cingulate epilepsy: Report of 3 electroclinical subtypes with surgical outcomes. *JAMA Neurology*, *70*, 995–1002.
- Amemiya, K., & Naito, E. (2016). Importance of human right inferior frontoparietal network connected by inferior branch of superior longitudinal fasciculus tract in corporeal awareness of kinesthetic illusory movement. *Cortex*, *78*, 15–30. <http://www.ncbi.nlm.nih.gov/pubmed/26986838>
- Azanon, E., Tamè, L., Maravita, A., Linkenauger, S. A., Ferrè, E. R., Tajadura-Jiménez, A., & Longo, M. R. (2016). Multimodal contributions to body representation. *Multisensory Research*, *29*, 635–661.
- Balanescu, B., Franklin, R., Ciurea, J., Mindruta, I., Rasina, A., Bobulescu, R. C., ... Barborica, A. (2014). A personalized stereotactic fixture for implantation of depth electrodes in stereoelectroencephalography. *Stereotactic and Functional Neurosurgery*, *92*, 117–125.
- Bär, K.-J., de la Cruz, F., Berger, S., Schultz, C. C., & Wagner, G. (2015). Structural and functional differences in the cingulate cortex relate to disease severity in anorexia nervosa. *Journal of Psychiatry & Neuroscience*, *40*, 269–279. <http://www.ncbi.nlm.nih.gov/pubmed/25825813>
- Bartolomei, F., Barbeau, E. J., Nguyen, T., McGonigal, A., Régis, J., Chauvel, P., & Wendling, F. (2012). Rhinal-hippocampal interactions during déjà vu. *Clinical Neurophysiology*, *123*, 489–495.
- Bartolomei, F., Lagarde, S., Médina Villalon, S., McGonigal, A., & Benar, C. G. (2017). The “Proust phenomenon”: Odor-evoked autobiographical memories triggered by direct amygdala stimulation in human. *Cortex*, *90*, 173–175. <http://linkinghub.elsevier.com/retrieve/pii/S0010945216303495>
- Bartolomei, F., Lagarde, S., Wendling, F., McGonigal, A., Jirsa, V., Guye, M., & Bénar, C. (2017). Defining epileptogenic networks: Contribution of SEEG and signal analysis. *Epilepsia*, *58*, 1131–1147. <https://doi.org/10.1111/epi.13791>
- Bernier, G. P., Richer, F., Giard, N., Bouvier, G., Merrier, M., Turmel, A., & Saint-Hilaire, J.-M. (1990). Electrical stimulation of the human brain in epilepsy. *Epilepsia*, *31*, 513–520. <https://doi.org/10.1111/j.1528-1157.1990.tb06099.x>
- Blakemore, S. J., Frith, C. D., & Wolpert, D. M. (1999). Spatio-temporal prediction modulates the perception of self-produced stimuli. *Journal of Cognitive Neuroscience*, *11*, 551–559. <http://www.ncbi.nlm.nih.gov/pubmed/10511643>
- Blanke, O. (2012). Multisensory brain mechanisms of bodily self-consciousness. *Nature Reviews Neuroscience*, *13*, 556–571. <https://doi.org/10.1038/nrn3292>
- Blanke, O., Landis, T., Seeck, M., & Roger, A. J. (2002). Stimulating illusory own-body perceptions. *Nature*, *419*, 269–270.
- Blanke, O., Landis, T., Spinelli, L., & Seeck, M. (2004). Out-of-body experience and autoscopia of neurological origin. *Brain*, *127*, 243–258.
- Cardinale, F., Cossu, M., Castana, L., Casaceli, G., Schiariti, M. P., Miserocchi, A., ... Lo Russo, G. (2013). Stereoelectroencephalography: Surgical methodology, safety, and stereotactic application accuracy in 500 procedures. *Neurosurgery*, *72*, 353–366.
- Caruana, F., Gerbella, M., Avanzini, P., Gozzo, F., Pelliccia, V., Mai, R., ... Rizzolatti, G. (2018). Motor and emotional behaviours elicited by electrical stimulation of the human cingulate cortex. *Brain*, *141*, 3035–3051.
- Chambon, V., Wenke, D., Fleming, S. M., Prinz, W., & Haggard, P. (2013). An online neural substrate for sense of agency. *Cerebral Cortex*, *23*, 1031–1037. <http://www.ncbi.nlm.nih.gov/pubmed/22510529>
- Colombet, B., Woodman, M., Badier, J. M., & Benar, C. G. (2015). AnyWave: A cross-platform and modular software for visualizing and processing electrophysiological signals. *Journal of Neuroscience Methods*, *242*, 118–126.
- Dale, A. M., Fischl, B., & Sereno, M. I. (1999). Cortical surface-based analysis: I. Segmentation and surface reconstruction. *NeuroImage*, *9*, 179–194. <http://www.sciencedirect.com/science/article/pii/S1053811998903950>
- de Vignemont, F. (2010). Body schema and body image--pros and cons. *Neuropsychologia*, *48*, 669–680. <http://linkinghub.elsevier.com/retrieve/pii/S0028393209003789>
- Destrieux, C., Fischl, B., Dale, A., & Halgren, E. (2010). Automatic parcellation of human cortical gyri and sulci using standard anatomical nomenclature. *NeuroImage*, *53*, 1–15. <http://www.sciencedirect.com/science/article/pii/S1053811910008542>
- Dewan, M. C., Shults, R., Hale, A. T., Sukul, V., Englot, D. J., Konrad, P., ... Naftel, R. P. (2017). Stereotactic EEG via multiple single-path omnidirectional trajectories within a single platform: Institutional experience with a novel technique. *Journal of Neurosurgery*, *129*, 1173–1181.
- Donos, C., Măliia, M. D., Mîndruță, I., Popa, I., Ene, M., Bălănescu, B., ... Barborica, A. (2016). A connectomics approach combining structural and effective connectivity assessed by intracranial electrical stimulation. *NeuroImage*, *132*, 344–358.
- Donos, C., Mîndruță, I., Ciurea, J., Măliia, M. D., & Barborica, A. (2016). A comparative study of the effects of pulse parameters for intracranial direct electrical stimulation in epilepsy. *Clinical Neurophysiology*, *127*, 91–101.
- Farrer, C., Frey, S. H., Van Horn, J. D., Tunik, E., Turk, D., Inati, S., & Grafton, S. T. (2008). The angular Gyrus computes action awareness representations. *Cerebral Cortex*, *18*, 254–261. <http://www.ncbi.nlm.nih.gov/pubmed/17490989>
- Fischl, B. (2012). FreeSurfer. *NeuroImage*, *62*, 774–781. <https://www.sciencedirect.com/science/article/pii/S1053811912000389?via%3Dihub>
- Fischl, B., Sereno, M. I., & Dale, A. M. (1999). Cortical surface-based analysis: II: Inflation, flattening, and a surface-based coordinate system. *NeuroImage*, *9*, 195–207. <http://www.sciencedirect.com/science/article/pii/S1053811998903962>

- Gallagher, S. (1986). Body image and body schema: A conceptual clarification. *The Journal of Mind and Behavior*, 7, 541–554. <https://www.jstor.org/stable/43853233>
- Gaudio, S., Wiemerslage, L., Brooks, S. J., & Schiöth, H. B. (2016). Neuroscience and biobehavioral reviews review article a systematic review of resting-state functional-MRI studies in anorexia nervosa: Evidence for functional connectivity impairment in cognitive control and visuospatial and body-signal integration. *Neuroscience and Biobehavioral Reviews*, 71, 578–589.
- Gloning, I., Gloning, K., Jellinger, K., & Tschabitscher, H. (1963). Über einen obduzierten fall von optischer körperschemastörung und héautoskopie. *Neuropsychologia*, 1, 217–231. <http://linkinghub.elsevier.com/retrieve/pii/0028393263900174>
- Graziano, M. S. A., & Botvinick, M. (2002). How the brain represents the body: Insights from neurophysiology and psychology. *Common Mechanisms in Perception and Action: Attention and Performance*, 19, 136–157.
- Hayes, D. J., Lipsman, N., Chen, D. Q., Woodside, D. B., Davis, K. D., Lozano, A. M., & Hodaie, M. (2015). Subcallosal cingulate connectivity in anorexia nervosa patients differs from healthy controls: A multi-tensor Tractography study. *Brain Stimulation*, 8, 758–768. <http://www.ncbi.nlm.nih.gov/pubmed/26073966>
- Heydrich, L., & Blanke, O. (2013). Distinct illusory own-body perceptions caused by damage to posterior insula and extrastriate cortex. *Brain*, 136, 790–803.
- Heydrich, L., Dieguez, S., Grunwald, T., Seeck, M., & Blanke, O. (2010). Illusory own body perceptions: Case reports and relevance for bodily self-consciousness. *Consciousness and Cognition*, 19, 702–710. <https://doi.org/10.1016/j.concog.2010.04.010>
- Ishida, H., Nakajima, K., Inase, M., & Murata, A. (2010). Shared mapping of own and others' bodies in visuotactile bimodal area of monkey parietal cortex. *Journal of Cognitive Neuroscience*, 22, 83–96. <http://www.ncbi.nlm.nih.gov/pubmed/19199418>
- Isnard, J., Taussig, D., Bartolomei, F., Bourdillon, P., Catenoix, H., Colnat-coulbois, S., ... Sauleau, P. (2018). French guidelines on stereoelectroencephalography (SEEG) Francine Chassoux i , Mathilde Chipaux c , Stéphane Clémenceau j. *Clinical Neurophysiology*, 48, 5–13.
- Jayakar, P., Gotman, J., Harvey, A. S., Palmini, A., Tassi, L., Schomer, D., ... Kahane, P. (2016). Diagnostic utility of invasive EEG for epilepsy surgery: Indications, modalities, and techniques. *Epilepsia*, 57, 1735–1747. <https://doi.org/10.1111/epi.13515>
- Kahane, P., & Landre, E. (2008). The epileptogenic zone. *Neurochirurgie*, 54, 265–271.
- Kahane, P., Minotti, L., Hoffmann, D., Lachaux, J.-P., & Ryvlin, P. (2003). Invasive EEG in the definition of the seizure onset zone: Depth electrodes. In *Handbook of clinical neurophysiology* (Vol. 3, pp. 109–133). Amsterdam: Elsevier.
- Keizer, A., Smeets, M. A. M., Dijkerman, H. C., Uzunbajakau, S. A., van Elburg, A., & Postma, A. (2013). Too fat to fit through the door: First evidence for disturbed body-scaled action in anorexia nervosa during locomotion. Ed. Manos Tsakiris. *PLoS One*, 8, e64602 <http://dx.plos.org/10.1371/journal.pone.0064602>
- Koubeissi, M. Z., Bartolomei, F., Beltagy, A., & Picard, F. (2014). Electrical stimulation of a small brain area reversibly disrupts consciousness. *Epilepsy & Behavior*, 37, 32–35. <https://doi.org/10.1016/j.yebeh.2014.05.027>
- Kravitz, D. J., Saleem, K. S., Baker, C. I., Ungerleider, L. G., & Mishkin, M. (2013). The ventral visual pathway: An expanded neural framework for the processing of object quality. *Trends in Cognitive Sciences*, 17, 26–49. <https://doi.org/10.1016/j.tics.2012.10.011>
- Lee, S., Ran, K., Ku, J., Lee, J., Namkoong, K., & Jung, Y. (2014). Resting-state synchrony between anterior cingulate cortex and precuneus relates to body shape concern in anorexia nervosa and bulimia nervosa. *Psychiatry Research: Neuroimaging*, 221, 2013–2015.
- Matsumoto, R., Kunieda, T., & Nair, D. (2017). Single pulse electrical stimulation to probe functional and pathological connectivity in epilepsy. *Seizure*, 44, 27–36.
- Mazzoni, L. N., Rotella, F., Faravelli, C., Pupi, A., Ricca, V., & Pellicano, G. (2013). Looking at my body. Similarities and differences between anorexia nervosa patients and controls in body image visual processing. *European Psychiatry*, 28, 427–435.
- Mcfadden, K. L., Tregellas, J. R., Shott, M. E., & Frank, G. K. W. (2014). Reduced salience and default mode network activity in women with anorexia nervosa. *Journal of Psychiatry & Neuroscience*, 39, 178–188.
- Mühlau, M., Gaser, C., Ilg, R., Conrad, B., Leibl, C., Cebulla, M. H., ... Nunnemann, S. (2007). Gray matter decrease of the anterior cingulate cortex in anorexia nervosa. *The American Journal of Psychiatry*, 164, 1850–1857. <http://www.ncbi.nlm.nih.gov/pubmed/18056240>
- Munari, C., & Bancaud, J. (1987). The role of stereo-electro-encephalography (SEEG) in the evaluation of partial epileptic patients. In R. J. Porter & P. L. Morselli (Eds.), *The epilepsies* (pp. 267–306). London: Butterworths.
- Munari, C., Hoffmann, D., Francione, S., Kahane, P., Tassi, L., Russo, G. L., & Benabid, A. L. (1994). Stereo-electroencephalography methodology: Advantages and limits. *Acta Neurologica Scandinavica*, 89, 56–67. <https://doi.org/10.1111/j.1600-0404.1994.tb05188.x>
- Munari, C., Kahane, P., Tassi, L., Francione, S., Hoffmann, D., Lo Russo, G., & Benabid, A. L. (1993). Intracerebral low frequency electrical stimulation: A new tool for the definition of the “epileptogenic area”? *Acta Neurochirurgica. Supplementum (Wien)*, 58, 181–185. <http://www.ncbi.nlm.nih.gov/pubmed/8109287>
- Murata, A., Wen, W., & Asama, H. (2016). The body and objects represented in the ventral stream of the parieto-premotor network. *Neuroscience Research*, 104, 4–15. <http://www.ncbi.nlm.nih.gov/pubmed/26562332>
- Murray, R. J., Fox, P. T., Bzdok, D., Debban, M., & Eickhoff, S. B. (2014). Functional connectivity mapping of regions associated with self- and other-processing. *Human Brain Mapping*, 36, 1304–1324.
- Nightingale, S. (1982). Somatoparaphrenia: A case report. *Cortex*, 18, 463–467. <http://linkinghub.elsevier.com/retrieve/pii/S0010945282800439>
- Northoff, G., & Bermpohl, F. (2004). Cortical midline structures and the self. *Trends in Cognitive Sciences*, 8, 102–107.
- Northoff, G., Heinzel, A., De Greck, M., Bermpohl, F., Dobrowolny, H., & Panksepp, J. (2006). Self-referential processing in our brain—A meta-analysis of imaging studies on the self. *NeuroImage*, 31, 440–457.
- Parvizi, J., Rangarajan, V., Shirer, W., Desai, N., & Michael, D. (2014). The will to persevere induces by electrical stimulation of the human cingulate gyrus. *Neuron*, 80, 1359–1367.
- Picard, F., Scavarda, D., & Bartolomei, F. (2013). Induction of a sense of bliss by electrical stimulation of the anterior insula. *Cortex*, 49, 2935–2937.
- Qin, P., & Northoff, G. (2011). NeuroImage how is our self related to midline regions and the default-mode network? *NeuroImage*, 57, 1221–1233.
- Quraishi, I. H., Benjamin, C. F., Spencer, D. D., Blumenfeld, H., & Alkawadri, R. (2017). Impairment of consciousness induced by bilateral electrical stimulation of the frontal convexity. *Epilepsy Behav Case Reports*, 8, 117–122.
- Richer, F., Martinez, M., Robert, M., Bouvier, G., & Saint-Hilaire, J. M. (1993). Stimulation of human somatosensory cortex: Tactile and body displacement perceptions in medial regions. *Experimental Brain Research*, 93, 173–176. <http://www.ncbi.nlm.nih.gov/pubmed/8467887>
- Rizzolatti, G., Fabbri-Destro, M., Caruana, F., & Avanzini, P. (2018). System neuroscience: Past, present, and future. *CNS Neuroscience & Therapeutics*, 24, 685–693.
- Rodgers, K. M., Benison, A. M., Klein, A., & Barth, D. S. (2008). Auditory, somatosensory, and multisensory insular cortex in the rat. *Cerebral Cortex*, 18, 2941–2951. <https://www.ncbi.nlm.nih.gov/pmc/articles/PMC2583160/pdf/bhn054.pdf>
- Rubinov, M., & Sporns, O. (2010). Complex network measures of brain connectivity: Uses and interpretations. *NeuroImage*, 52, 1059–1069. <https://doi.org/10.1016/j.neuroimage.2009.10.003>
- Schwarzlose, R. F. (2005). Separate face and body selectivity on the fusiform Gyrus. *The Journal of Neuroscience*, 25, 11055–11059. <http://www.jneurosci.org/cgi/doi/10.1523/JNEUROSCI.2621-05.2005>
- Sherrington, C. S. (1911). *The integrative action of the nervous system*. New Haven: Yale University Press <http://content.apa.org/books/13798-000>
- Thurm, B. E., Pereira, E. S., Fonseca, C. C., Cagno, M. J. S., & Gama, E. F. (2011). Neuroanatomical aspects of the body awareness. *Journal of Morphological Science*, 28, 296–299.
- Trebuchon, A., & Chauvel, P. (2016). Electrical stimulation for seizure induction and functional mapping in Stereoelectroencephalography. *Journal of Clinical Neurophysiology*, 33, 511–521.

- Tsakiris, M., Hesse, M. D., Boy, C., Haggard, P., & Fink, G. R. (2007). Neural signatures of body ownership: A sensory network for bodily self-consciousness. *Cerebral Cortex*, *17*, 2235–2244.
- Wendling, F., Bartolomei, F., Bellanger, J. J., & Chauvel, P. (2001). Interpretation of interdependencies in epileptic signals using a macroscopic physiological model of the EEG. *Clinical Neurophysiology*, *112*, 1201–1218. <http://www.ncbi.nlm.nih.gov/pubmed/11516732>
- Winkler, A. M., Sabuncu, M. R., Yeo, B. T. T., Fischl, B., Greve, D. N., Kochunov, P., ... Glahn, D. C. (2012). Measuring and comparing brain cortical surface area and other areal quantities. *NeuroImage*, *61*, 1428–1443.
- Yu, H., Pistol, C., Franklin, R., & Barborica, A. (2018). Clinical accuracy of customized stereotactic fixtures for Stereoelectroencephalography. *World Neurosurgery*, *109*, 82–88. <http://www.sciencedirect.com/science/article/pii/S1878875017315966>
- Yu, K., Liu, C., Yu, T., Wang, X., Xu, C., Ni, D., & Li, Y. (2018). Out-of-body experience in the anterior insular cortex during the intracranial electrodes stimulation in an epileptic child. *Journal of Clinical Neuroscience*, *54*, 122–125.
- Zu Eulenburg, P., Best, C., Müller-Forell, W., Baier, B., Geber, C., Müller-Forell, W., ... Dieterich, M. (2013). Posterior insular cortex-site of

vestibular-somato sensory interaction? Vestibular migraine view project autoimmune mechanisms in a mouse model of complex regional pain syndrome view project posterior insular cortex-a site of vestibular-somatosensory interaction? *Brain and Behavior: A Cognitive Neuroscience Perspective*, *3*, 519–524. <https://www.researchgate.net/publication/259589672>

SUPPORTING INFORMATION

Additional supporting information may be found online in the Supporting Information section at the end of this article.

How to cite this article: Popa I, Barborica A, Scholly J, et al. Illusory own body perceptions mapped in the cingulate cortex—An intracranial stimulation study. *Hum Brain Mapp*. 2019; 40:2813–2826. <https://doi.org/10.1002/hbm.24563>